The Journal of Laryngology and Otology
June 1999, Vol. **113**, pp. 501–508

Review Article

The suprahyoid neck: normal and pathological anatomy

V. F. H. Chong, M.B.B.S., F.R.C.R.*, S. K. Mukherji, M.D.†, C. H. K. Goh, M.B.B.S., F.R.C.S.‡

Abstract
The suprahyoid neck can be divided into fascia-bound spaces. These spaces, which are readily demonstrated on computed tomography (CT) and magnetic resonance imaging (MRI), form the anatomical framework for generating differential diagnosis and assessing disease extent. By correlating the radiological features with clinical information, the diagnostic possibilities of demonstrated lesions could be narrowed down considerably. Multiple space involvement is common in inflammatory and neoplastic processes and the full extent of these lesions should be outlined to facilitate surgical or radiotherapy planning.

Introduction

The concept of dividing the extracranial head and neck into spaces dates back to the 1800s. Anatomists and surgeons originally studied the fascial compartments to explain why infections spread in certain defined ways (Grodinsky and Holyoke, 1938). Over the years, anatomists and surgeons have adopted the organization of the head and neck into fascial compartments but this approach was not commonly used by radiologists until the late eighties and early nineties. However, the radiological terminology may not be the same as that used by surgeons or anatomists. Although anatomists pioneered the work on fascia anatomy and spaces, they have not widely incorporated the clinically used scheme into the standard textbooks of anatomy (Bannister *et al.*, 1995).

This paper focuses on spaces of the suprahyoid neck and shows how they can be used to formulate differential diagnosis, assess disease extent, and facilitate surgical or radiotherapy planning.

Spaces of the suprahyiod neck

The basis for dividing the suprahyoid neck into spaces is the arrangement of the cervical fascia, which consists of two layers: the superficial and deep cervical fascia. The superficial cervical fascia consists of the subcutaneous tissues and the deep cervical fascia has three components – the superficial, middle layer and deep layers. It is the reflections of these components of the deep cervical fascia that define the spaces of the suprahyoid neck.

When imaging detects a lesion, the first task is to localize it to one of the spaces. This is important as each space has sufficiently different contents to produce unique lesions. The morphology of a lesion, together with clinical information, often helps to narrow considerably the list of diagnostic possibilities. In most instances, a lesion is centred within the space of origin and locating the site of origin is not a difficult exercise. However, when a lesion is large and encroaches on adjacent spaces, displacement of the parapharyngeal space (PPS) may give another clue to the origin of the abnormality.

Parapharyngeal space (PPS)

There is some confusion in the nomenclature used to describe the suprahyoid neck. The PPS is divided into two components by some authors (Lewin, 1995). In this system, the anterior prestyloid compartment is fat-filled while the posterior retrostyloid compartment contains the carotid sheath. However, other authors consider this retrostyloid compartment as a separate space termed the carotid space (CS) (Harnsberger and Osborn, 1991). The retrostyloid PPS is, therefore, the same as the CS.

The importance of the PPS is its central location and the relationship to the other spaces of the neck (Figure 1). The masticator space (MS) is located anterolaterally, the parotid space (PS) laterally, the visceral space (VS) medially, the CS posteriorly, and the retropharyngeal space (RPS) posteromedially. The PPS stretches from the skull base to the submandibular space inferiorly. The fat-filled PPS contains the pharyngeal venous plexus, branches of

From the Departments of Diagnostic Radiology* and Otolaryngology‡, Singapore General Hospital, Singapore and the Department of Radiology and Surgery†, University of North Carolina School of Medicine, Chapel Hill, NC, USA.
Accepted for publication: 13 February 1999.

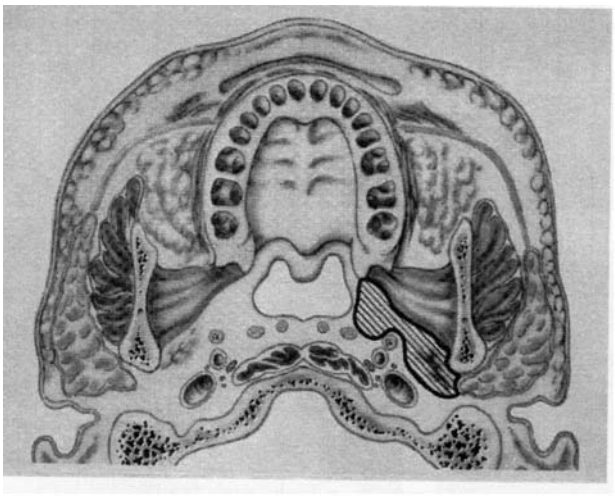

(a)

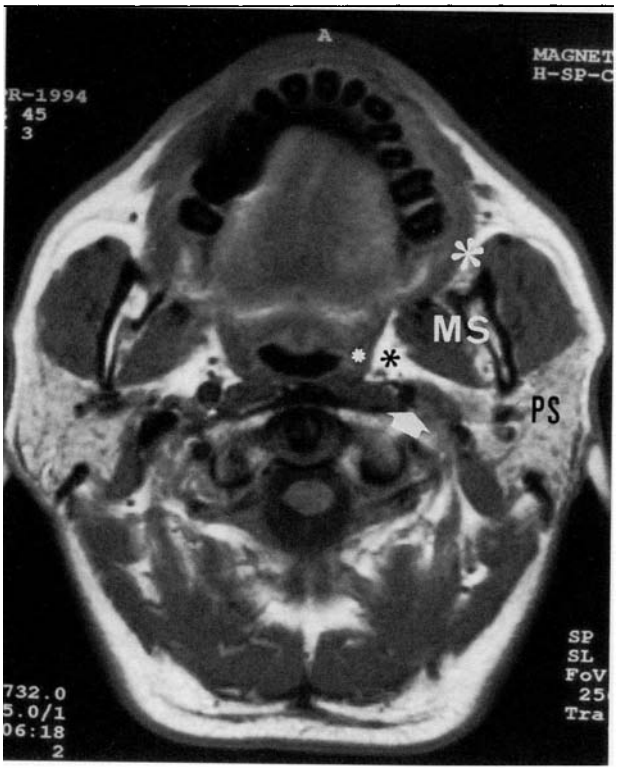

(b)

(c)

FIG. 1

Normal anatomy of PPS. 1a: Schematic illustration shows the location and extent of the left PPS. (Modified and reproduced with permission, Mukherji and Castillo, 1998). 1b: Axial T1-weighted MRI shows the left PPS (black asterisk) separating the masticator space (MS) from visceral space (small white asterisk). The carotid space (arrow) is located posteriorly and the parotid space (PS) laterally. Note the buccal space (large white asterisk). 1c: Coronal T1-weighted MRI shows right PPS (small asterisks) separating pharyngeal mucosa from the MS (MS). Note PPS is in contiguity with submandibular space (large asterisk).

the mandibular nerve, the internal maxillary artery and the ascending pharyngeal artery. The buccal space (BS), which is anterior to the MS, is not in contact with the PPS.

The differential diagnosis of PPS lesions is limited, reflecting the normal contents of this space. Congenital lesions involving the PPS include atypical second branchial cyst and lymphangiomas. Pleomorphic adenomas can arise from ectopic salivary glands and they form the most common group of primary PPS tumour. Malignant tumours arising from minor salivary glands are rare (Figure 2). By far, the most common malignant lesions in the PPS are due to infiltration from surrounding spaces.

Parotid space (PS)

The PS is located lateral to the PPS (Figure 1). Hence, a mass arising from the PS is expected to invade or displace the PPS from a lateral to medial direction. These lesions include abscesses, lymphomas, and primary or secondary parotid tumours. PS lesions are readily evaluated by clinical means.

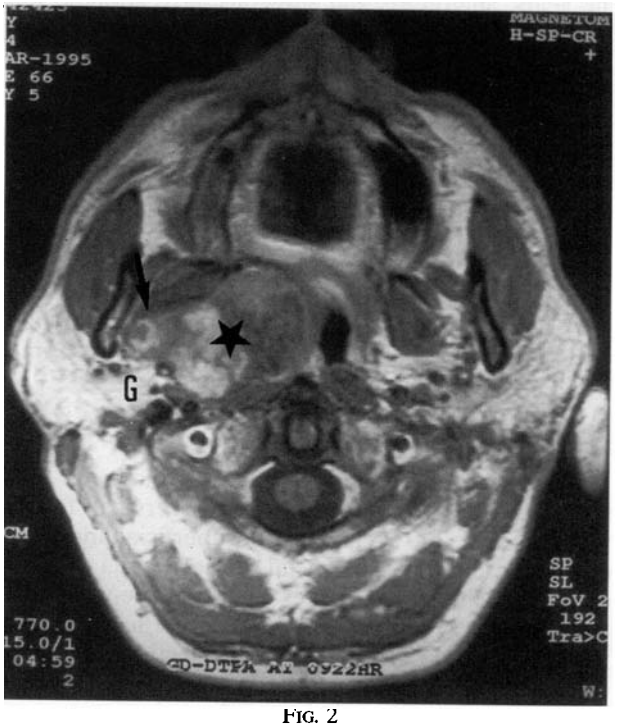

FIG. 2

Primary adenocystic carcinoma in PPS. Axial contrast-enhanced MRI shows a mixed signal intensity mass in the right PPS (star). Note infiltration of the medial pterygoid muscle (arrow). The mass is separated from the deep lobe of the parotid gland (G).

https://doi.org/10.1017/S0022215100144354 Published online by Cambridge University Press

These lesions can often be aspirated for cytological examinations and managed adequately without radiological studies. However, the extent of parotid disease should be assessed if deep lobe involvement is suspected. In addition, nasopharyngeal tumours can mimic a primary parotid lesion when it invades or displaces the parotid gland laterally (Wanamaker *et al.*, 1994).

It is particularly important to separate a tumour arising from the deep lobe of the parotid gland from a primary PPS salivary gland tumour (Figure 3). A primary PPS mass can be confidently diagnosed if a rim of parapharyngeal fat can be seen around lesion. However, this clue may not be seen as large lesions tend to efface the fat planes. A mass, which may be predominantly in the PPS but with a component in superficial lobe, is likely to have originated from the deep parotid lobe (Mukherji and Castillo, 1998).

Visceral space (VS)

The VS, which is enclosed by the visceral fascia, is also known as the pharyngeal mucosal space. Primary VS lesions are usually diagnosed endoscopically and confirmed with biopsy. Mucosal lesions are often clinically characteristic but radiologically may appear quite unremarkable. Imaging studies, not uncommonly, fail to identify these lesions. When they are seen radiologically, the mucosal extent is frequently underestimated. The primary role of imaging is in the assessment of deep infiltration.

Although the anatomy of the neck is divided into spaces, squamous cell carcinoma (SCCa) are more conveniently described and staged using the traditional subdivisions of the pharynx. SCCa commonly spread laterally into the PPS. In the nasopharynx, penetration of the pharyngobasilar fascia with subsequent spread to the PPS and beyond into the MS may lead to perineural infiltration of the mandibular nerve (Chong, 1996; Chong *et al.*, 1996a). Identifying parapharyngeal infiltration is important as a parapharyngeal boost is given during radiotherapy to control lateral spread (Sham *et al.*, 1991). Parapharyngeal spread also precludes surgery or brachytherapy.

The most commonly seen lesion arising from the VS is SCCa which accounts for 70 per cent of the malignancies (Mendenhall *et al.*, 1994). Lymphomas account for approximately 20 per cent and the remaining 10 per cent consist of a variety of lesions including adenocystic carcinoma, melanoma and rhabdomyosarcoma.

Masticator space (MS)

The superficial layer of the deep cervical fascia splits at the inferior margin of the mandible to envelop the MS (formerly known as the infratemporal fossa. The lateral sling covers the masseter muscle, continues superiorly to the zygomatic arch and covers the temporalis muscle. The medial sling covers the medial pterygoid muscle and inserts into the skull base. The muscles of mastication (temporalis, masseter, medial and lateral pterygoid) make up the bulk of the MS (Figure 4). Thereis no fascia dividing the suprazygomatic (temporal) portion from the infratemporal portion of the MS. Pathological processes may, therefore, show contiguous spread from the infrazygomatic portion of the MS to the suprazygomatic portion (Figure 5).

The most commonly seen lesions in the MS are due to inflammation and neoplasm (Figure 5). Infection of the MS from an odontogenic abscess is not uncommon. Primary neoplasms are less commonly seen but include malignant bone tumours and soft tissue sarcomas such as malignant fibrohistiocytoma (Chong and Fan, 1996a).

FIG. 3

Deep lobe parotid pleomorphic adenoma. Axial contrast-enhanced MRI shows a large mass arising from the deep lobe of the left parotid gland displacing the medial pterygoid muscle (arrowheads) anteriorly and extending into the superficial lobe (arrow).

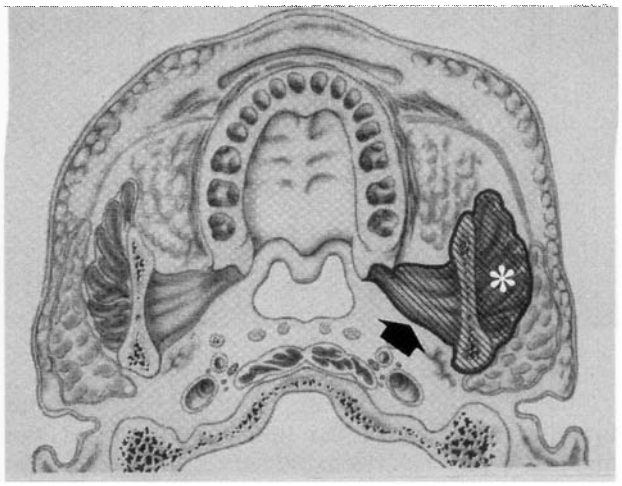

FIG. 4

Schematic illustration shows the left MS (cross-hatched). Note the medial pterygoid muscle (arrow) and the masseter muscle (asterisk). (Modified and reproduced with permission, Mukherji and Castillo, 1998).

https://doi.org/10.1017/S0022215100144354 Published online by Cambridge University Press

(a)

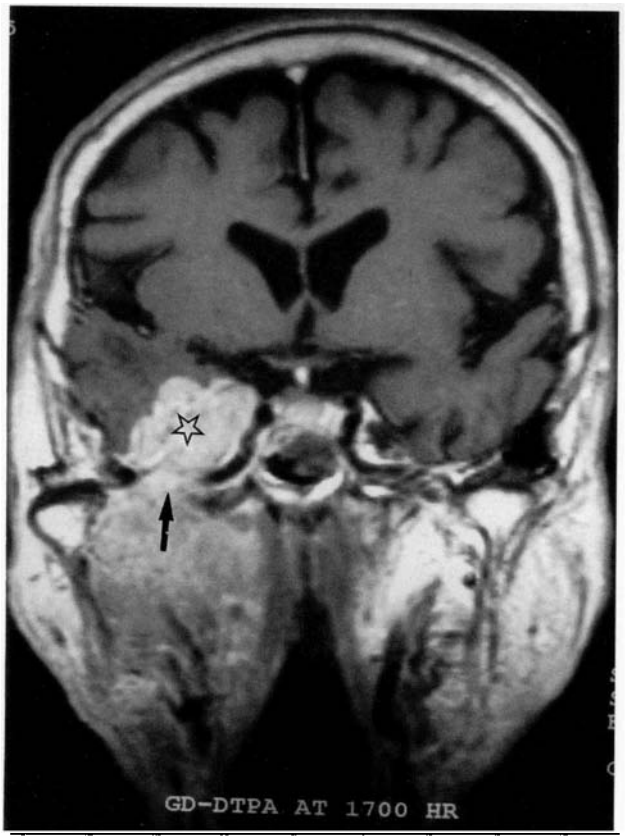

(b)

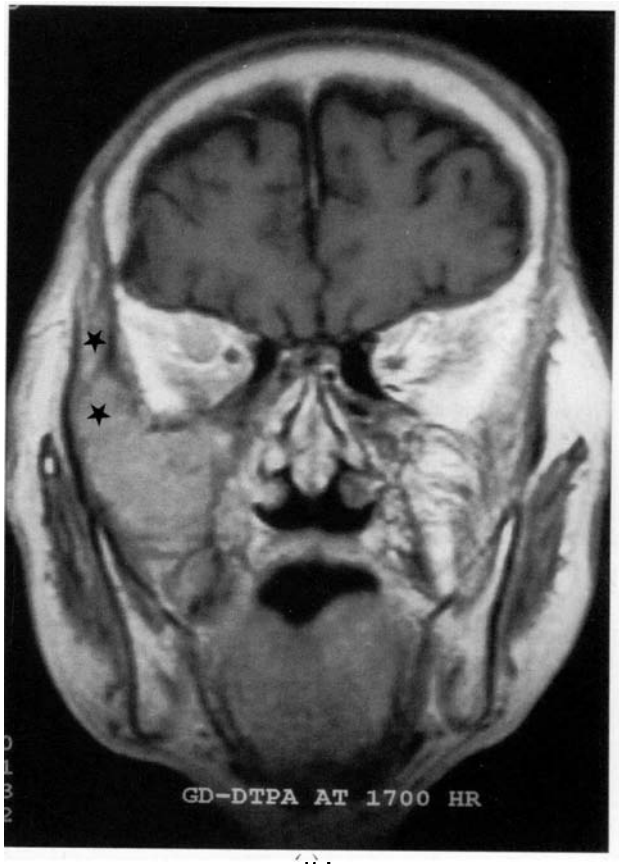

(c)

FIG. 5

MS malignant fibrohistiocytoma. 5a: Axial CT shows a right MS mass (asterisk). Note the normal left medial pterygoid muscle (stars). 5b: Coronal contrast-enhanced MRI (four months later) shows tumour extending into the right middle cranial fossa (star) via the foramen ovale (arrow). 5c: Coronal contrast-enhanced MRI shows tumour extension into the suprazygomatic portion of the MS (stars).

The mandibular nerve enters the MS through the foramen ovale. It gives rise to two motor nerves, the masticator and the mylohyoid nerves. The masticator nerve supplies the muscles of mastication. The mylohyoid nerve innervates the mylohyoid and anterior belly of the digastric muscles that are located in the floor of the mouth. Injury to these nerves result in muscle atrophy (Figure 6).

Buccal space (BS)

The BS has received limited attention in the radiological literature (Braun and Hoffman, 1984; Tart *et al.*, 1995). It is bordered medially by the buccinator muscle and the maxillary alveolar ridge, and posterolaterally by the MS. Anteriorly, the BS is separated from the subcutaneous tissues by the muscles of facial expression. Inferiorly, the BS blends with the submandibular space. The BS consists of mainly fat but also contains minor salivary gland tissue, parotid duct, lymph nodes, facial vein, facial (angular) and buccal artery, buccal branch of the facial nerve, and the buccal division of the mandibular nerve.

The most common lesion in the BS is infiltration from buccal SCCa. Primary lesions are uncommon and they include sebaceous cysts, lipomas, and haemangiomas (Figure 7). A dilated parotid duct, which is usually due to a stone in the orifice of Stenson's duct, or accessory parotid tissue can also present as a BS mass.

Carotid space (CS)

The CS, also referred to as the carotid sheath, contains the carotid artery, the internal jugular vein, cranial nerves, sympathetic plexus and lymph nodes

https://doi.org/10.1017/S0022215100144354 Published online by Cambridge University Press

(a)

(b)

FIG. 6

Denervation atrophy muscles of mastication. 6a: Axial T1-weighted MRI shows atrophy of the right medial pterygoid (arrowheads) and masseter (arrow) muscles. Note the normal left medial pterygoid muscle (asterisk) and masseter muscle (star). 6b: Coronal contrast-enhanced MRI shows tumour involvement of the right mandibular nerve (arrow) and cavernous sinus (small asterisks). Note the normal left medial (small star) and lateral (large) pterygoid muscles. There is atrophy of the right medial pterygoid muscle (large asterisk).

(Figure 8). Abnormalities in the CS often show features suggesting their histological diagnosis. These lesions may compress the PPS anteriorly, displace the parotid gland laterally, and characteristically splay the vessels of the carotid sheath (Figure 9).

Two types of tumours can arise from CS nerves, schwannomas are encapsulated benign tumours originating from Schwann cells surrounding the nerves. In contrast, neurofibromas are nonencapsu-

FIG. 7

Buccal space (BS) haemangioma. T2-weighted MRI shows high signals and good delineation of haemangioma. Note a smaller lesion anteriorly (arrow).

lated and contain all elements of the nerve of origin. Neurofibromas show low attentuation on CT as a result of the rich lipid content and they may not show appreciable contrast enhancement. The low density (near water) on CT is a characteristic (Fruin *et al.*, 1990). On MRI, neurofibromas appear similar to schwannomas (Figure 10). Although neurofibromas are lipid-rich, T1-weighted MRI does not show an increase in signal intensity.

Paragangliomas are found in relation to the CS. Glomus jugulare may cause variable erosion of the

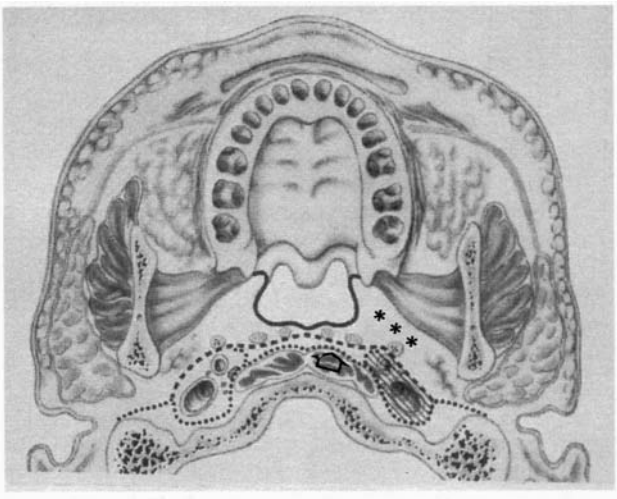

FIG. 8

Schematic illustration shows the right CS (cross-hatched), the RPS (hollow arrow) and the left PPS (asterisks). (Modified and reproduced with permission, Mukherji and Castillo, 1998).

https://doi.org/10.1017/S0022215100144354 Published online by Cambridge University Press

FIG. 9

Bilateral glomus vagale. Axial T2-weighted MRI shows high signal intensity left glomus vagale displacing the external carotid anteriorly (arrow), the internal carotid posteriorly (arrowhead) and the internal jugular vein laterally (asterisk). Note the smaller tumour on the right (star).

jugular foramen and typically produces a permeative pattern of destruction (Chong and Fan, 1996b). This is in contrast to neurofibromas or schwannomas which charateristically cause a smooth scalloped appearance. Paragangliomas are highly vascular and enhances intensely on CT. They can be differentiated from schwannomas or neurofibromas on MRI imaging when the typical 'salt and pepper' appearance is present.

Lymph nodes with extracapsular spread may infiltrate the CS. Unfortunately, radiological diagnosis of vascular infiltration is often difficult. Even when the CS is almost surrounded by tumour, the arterial adventitia may be free at surgery. On the other hand, a small area of tumour contact may result in adventitia infiltration. CT is superior to MRI in the identification of extracapsular spread and nodal necrosis (Yousem *et al.*, 1992; Chong *et al.*, 1996b).

Thrombosis of the internal jugular vein is usually seen in patients with previous central venous line insertion, drug abuse or malignancy. There is enlargement of the thrombus filled vein surrounded by a rim of enhancing vessel wall (Figure 11). Thrombosis of the internal jugular vein may be easily confused with a necrotic lymph node or an abscess if contiguous sections are not examined. A thrombosed internal jugular vein is seen as a tubular structure but an abscess or necrotic node retains a rounded configuration.

(a)

(b)

FIG. 10

Sympathetic plexus neurofibroma. 10a: Axial contrast-enhanced CT shows a low density lesion (star) displacing the external carotid artery anteriorly (small arrowhead). The internal carotid artery and the internal jugular vein are displaced posterolaterally (large arrowhead). 10b: Axial contrast-enhanced MRI shows a heterogeneous enhancement pattern.

The carotid artery may deviate medially mimicking a submucosal mass clinically. The patient illustrated in Figure 12 went to his family physician because of a vague lump in his neck. He was subsequently referred to an otolaryngologist. A

https://doi.org/10.1017/S0022215100144354 Published online by Cambridge University Press

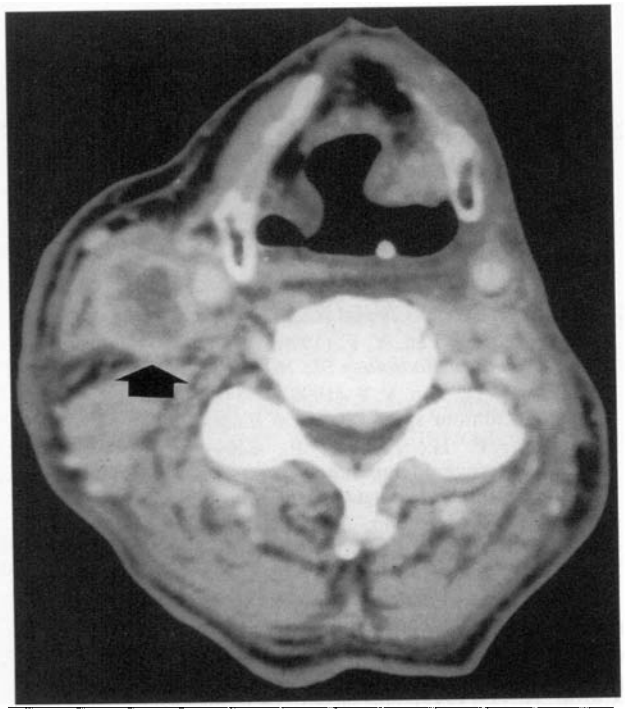

FIG. 11

Thrombosed internal jugular vein. Axial contrast-enhanced CT shows an enlarged thrombosed right internal jugular vein (arrow). Note previous left radical neck dissection.

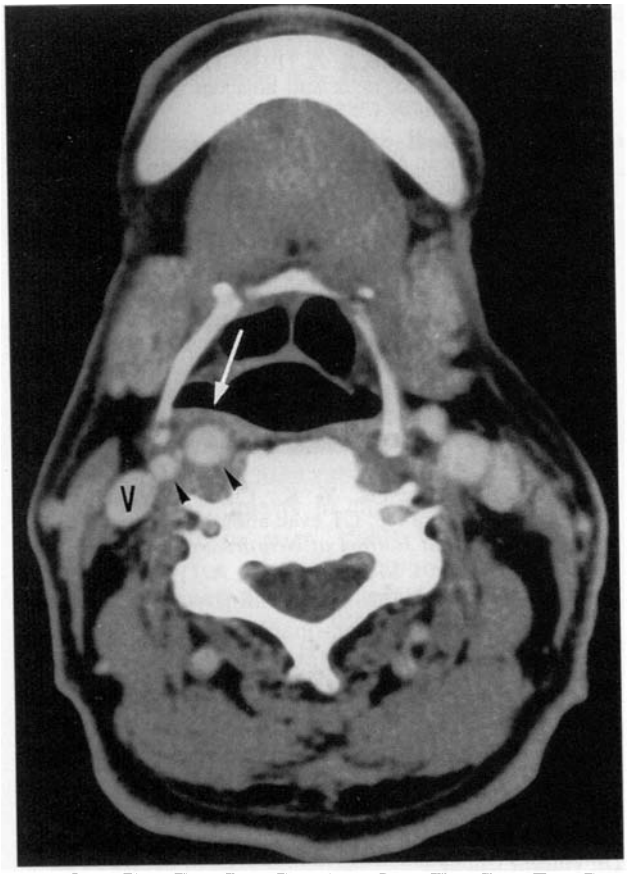

FIG. 12

Pseudolesion in CS. Axial contrast-enhanced CT shows medially deviated carotid artery just superior to the bifurcation (arrowheads) mimicking a pulsatile supraglottic mass. Note the internal jugular vein (V) and the bulging posterior pharyngeal wall (arrow).

bulging pulsatile 'mass' was noted in the right pyriform sinus. CT showed a medially deviated internal carotid artery deforming the pyriform sinus posteriorly.

Retropharyngeal space (RPS)

The RPS is a potential space that extends from the skull base to approximately T4. This space is situated between the pharyngeal constrictor muscles anteriorly and the prevertebral muscles posteriorly. The alar fascia, a slip of the deep cervical fascia, forms the lateral wall of the RPS. A median raphe divides this space into two halves. There are up to three nodes on each side of the RPS (Chong *et al.*, 1995). These nodes are usually located on the longus colli muscle between the CS and the VS. When enlarged, they displace the PPS anteriorly.

The two principal disease processes in the RPS are infection and malignancy. The palatine tonsils and the nasopharyngeal adenoids are important original sites of infection (Gates, 1996). Organisms spreading to the lateral retropharyngeal (LRP) nodes may result in suppurative lymphadenopathy. The RPS is a potential conduit for the spread of infection from the neck to the posterior mediastinum. Tuberculous spondylitis may decompress into the prevertebral space and subsequently into the RPS (Figure 13).

There are no primary tumours in the RPS. Malignant lesions are mostly due to LRP nodal metastasis or SCCa originating from the adjacent VS

FIG. 13

Spinal tuberculosis with retropharygneal abscess. Axial contrast-enhanced CT shows spinal tuberculosis decompressing into the PVS (arrow) and the right RPS (cross).

https://doi.org/10.1017/S0022215100144354 Published online by Cambridge University Press

(Figure 14) (Curtin, 1991). Oropharyngeal SCCa can also spread superiorly within the RPS to reach the skull base resulting in bone destruction (Chong and Fan, 1998).

Prevertebral space (PVS)

The PVS, which is enclosed by the prevertebral fascia, is posterior to the RPS. Primary PVS masses typically displace the RPS and the posterior wall of the visceral space anteriorly and the carotid sheath laterally. Vertebral body involvement is a conclusive sign of PVS involvement. The contents of the PVS in the suprahyoid neck are the longus colli muscle, vertebral bodies and discs, spinal canal, vertebral artery, and phrenic nerve.

Primary malignant lesions in the prevertebral muscles are uncommon. However, invasion from an adjacent nasopharyngeal SCCa is not unusual. The vertebral bodies are frequent sites for metastatic disease. Pyogenic or tuberculous infection of the cervical spine can also be seen from time to time (Figure 14).

In conclusion, the suprahyoid neck can be divided into distinct spaces with their own differential diagnosis. By observing the centre of the lesion and the direction of displacement or infiltration of the PPS, it is possible to localize a lesion to one of these spaces. The location, together with the radiological features can often help to predict the histological diagnosis. Infection and malignant neoplasms can affect multiple spaces and the disease extent should be demonstrated for treatment planning.

FIG. 14

Metastatic retropharyngeal lymphadenopathy. Axial contrast-enhanced CT shows a large necrotic right retropharyngeal node (asterisk). The primary tumour was a tonsillar SCCa.

References

Bannister, L. H., Berry, M. M., Collins, P., Dyson, M., Dussek, J. E., Ferguson, M. W. J. (1995) *Grays Anatomy*. Churchill Livingston, Edinburgh.

Braun, I. F., Hoffman, J. C. (1984) Computed tomography of the buccomaseteric region. *American Journal of Neuroradiology* **5:** 605–610.

Chong, V. F. H. (1996) Trigeminal neuralgia in nasopharyngeal carcinoma. *Journal of Laryngology and Otology* **110:** 394–396.

Chong, V. F. H., Fan, Y. F. (1996a) Radiology of the masticator space. *Clinical Radiology* **51:** 457–465.

Chong, V. F. H., Fan, Y. F. (1996b) Radiology of the carotid space. *Clinical Radiology* **51:** 762–768.

Chong, V. F. H., Fan, Y. F. (1998) The retropharyngeal space: route of tumour spread. *Clinical Radiology* **53:** 64–67.

Chong, V. F. H., Fan, Y. F., Khoo, J. B. K. (1995) Retropharyngeal lymphadenopathy in nasopharyngeal carinoma. *European Journal of Radiology* **21:** 100–105.

Chong, V. F. H., Fan, Y. F., Khoo, J. B. K. (1996a) Nasopharyngeal carcinoma with intracranial spread: CT and MR characteristics. *Journal of Computer Assisted Tomography* **20:** 563–569.

Chong, V. F. H., Fan, Y. F., Khoo, J. B. K. (1996b) MRI features of cervical nodal necrosis in metastatic disease. *Clinical Radiology* **51:** 103–109.

Curtin, H. D. (1991) The larynx. In *Head and Neck Imaging* (Som, P. M., Bergeron, R. T., eds.) 2nd Edition. Mosby Year Book, pp 593–692.

Fruin, M. E., Smoker, W. R. K., Harnsberger, H. R. (1990) The carotid space in the suprahyoid neck. *Seminars in Ultrasound, CT and MR* **11:** 504–519.

Gates, G. A. (1996) Sizing up the adenoids. *Archives of Otolaryngology – Head and Neck Surgery* **122:** 239–240.

Grodinsky, M., Holyoke, E. A. (1938) The fasciae and fascial spaces of the head, neck and adjacent regions. *American Journal of Anatomy* **63:** 367–408.

Harnsberger, H. R., Osborn, A. G. (1991) Differential diagnosis of head and neck lesions based on their space of origin. 1. The suprahyoid part of the neck. *American Journal of Roentgenology* **157:** 147–154.

Lewin, J. S. (1995) Imaging the suprahyoid neck. In *Imaging of the Head and Neck*. (Valvassori, G. E., Mafee, M. F., Carter, B. L., eds.) Thieme, New York, pp 390–423.

Mendenhall, W. M., Million, R. R., Mancuso, A. A., Stringer, S. P. (1994) Nasopharynx. In *Management of Head and Neck Cancer: A Multidisciplinary Approach*. (Million, R. R., Cassisi, N. J., eds.) Lippincott, Philadelphia pp 599–626.

Mukherji, S. K., Castillo, M. (1998) A simplified approach to spaces of the suprahyoid neck. *Radiologic Clinics of North America* **36:** 761–780.

Sham, J. T. S., Cheung, Y. K., Choy, D. (1991) Nasopharyngeal carcinoma: CT evaluation of patterns of tumor spread. *American Journal of Neuroradiology* **12:** 265–270.

Tart, R. P., Kotzur, I. M., Mancuso, A. A. (1995) CT and MR imaging of the buccal space and buccal space masses. *Radiographics* **15:** 531–550.

Wanamaker, J. R., Kraus, D. H., Biscotti, C. V., Eliachar, I. (1994) Undifferentiated nasopharyngeal carcinoma presenting as a parotid mass. *Head and Neck* **16:** 589–593.

Yousem, D. M., Som, P. M., Hackney, D. B. (1992) Central nodal necrosis and extracapsular neoplastic spread in cervical lymph nodes: MR imaging versus CT. *Radiology* **182:** 753–759.

Address for correspondence:
Dr Vincent Chong,
Department of Diagnostic Radiology,
Outram Road,
Singapore 169608,
Republic of Singapore.

Fax: 65 3265031 or 65 2241407
e-mail: gdrcfh@sgh.gov.sg

https://doi.org/10.1017/S0022215100144354 Published online by Cambridge University Press